RESPIRATION PATTERN RECOGNITION USING DUAL TRI-AXIS ACCELEROMETERS

by

İbrahim Savruk

B.S., Electrical and Electronics Engineering, Marmara University, 2016

Submitted to the Institute for Graduate Studies in
Science and Engineering in partial fulfillment of
the requirements for the degree of
Master of Science

Graduate Program in Electrical and Electronics Engineering
Boğaziçi University

2021

ACKNOWLEDGEMENTS

Firstly, I would like to express my sincere and greatest graditude to my thesis supervisors Prof. Zeynep Yasemin Kahya for giving this interesting and precious topic and her great supports. Her advices help me to complete this thesis and it has been an honor for me to be her master student. I also want to thank thesis committee members, Prof. Oğuzhan Çiçekoğlu and Assist. Prof. İpek Şen for their comments for future directions.

I am very thankfull to Inofab Health and its co-founder Kerem Yaşar for his help. I completed my tests with SpiroHome Personal spirometer. His contributions help me to compare my results with spirometer which is compatible with ATS/ERS standards. I also would like to thank my friends Mustafa Kurt and Sinem Deniz Yenen for their supports for my thesis.

Finally my special thanks go to my family and my dear wife Semanur Savruk. I would not be able to write this thesis without their motivation and encouragement.

ABSTRACT

RESPIRATION PATTERN RECOGNITION USING DUAL TRI-AXIS ACCELEROMETERS

In this study, respiration pattern is extracted using chest movements. Two accelerometers are used to track chest movements. Accelerometers are placed on the right side of the chest and the dorsal as mirror symmetrical not to be affected by heart beats. The data read from the accelerometer with the microprocessor is transferred to the MATLAB software by wireless communication. Bluetooth is used as a wireless communication method. Respiration pattern is extracted from the data by applying digital filter and axis fusion. Third order low pass Butterworth filter with 0.5 Hz cutoff frequency is applied to accelerometer axes data to eliminate noise. Respiration rate is calculated using filtered data. Results are compared with spirometer which is the golden standard for flow and volume measurements. Correlation coefficient, SKLD(Symmetric Kullback-Leibler Distance) and mean delay values are calculated besides comparing the graphical representations. Validation and comparison tests are applied with two scenarios which are tests on non-moving body and tests on moving body. According to results, 260 ms mean delay, 0.8280 mean correlation coefficient per respiration cycle and 0.7786 correlation coefficient per non-moving tests are calculated when results are compared with spirometer. In the second part of the study, respiration pattern has been tried to be extracted in moving body. The results are compared with spirometer. Tests are repeated with rotational and reciprocating movements. 583 ms mean delay, 0.6845 mean correlation coefficient per respiration cycle and 0.5861 correlation coefficient for per tests are calculated in these tests.

ÖZET

ÜÇ EKSENLİ İKİ AKSELEROMETRE KULLANARAK SOLUNUM MOTİFİ ÇIKARIMI

Bu çalışmada, göğüs hareketlerinden faydalanılarak solunum motifi çıkarılmıştır. Göğüs hareketlerinin izlenilebilmesi için, iki adet akselerometre kullanılmıştır. Akselerometreler kalp atışlarından etkilenmemesi için göğüsün ve sırtın sağ taraflarına ayna simetrik olarak yerleştirilmiştir. Akselerometreden mikroişlemci ile okunan veriler kablosuz haberleşme ile MATLAB yazılımına aktarılmıştır. Kablosuz haberleşme yöntemi olarak Bluetooth kullanılmıştır. Aktarılan veriye dijital filtreler ve eksen birleştirmesi uygulanarak solunum motifi çıkarılmıştır. Akselerometre verilerinde oluşan gürültüyü elemek için sinyale 0.5 Hz kesmeli üçüncü derece butterworth alçak geçirgen filtre uygulanmıştır. Elde edilen sonuçlar kullanılarak solunum oranı hesaplanmıştır. Verilerin doğruluğunu hesaplayabilmek için altın standart olan spirometre cihazı ile karşılaştırmalar yapılmıştır. Grafik benzerliğinin yanı sıra korelasyon katsayısı, SKLD (Simetrik Kullback-Leibler Mesafesi) değerleri ve ortalama gecikme değerleri hesaplanarak sayısal benzerlikler bulunmuştur. Testler hareketli vücut ve sabit vücutta olmak üzere 2 ayrı senaryo ile yapılmıştır. Elde edilen sonuçlara göre ortalama 280 ms gecikme, soluk başına ortalama 0.8280 ve test başına ortalama 0.7786 korelasyon değeri hesaplanmıştır. Çalışmanın ikinci kısmında, literatür çalışmalarından farklı olarak hareketli bir vücutta solunum motifi çıkarılmaya çalışılmıştır. Elde edilen sonuçlar spirometre ile kıyaslanmıştır. Testler dairesel, periyodik vücut hareketleri ile tekrarlanmıştır. Bu testler sonucunda soluk başına 0.6845, test başına 0.5861 korelasyon katsayısı ve ortalama 583 milisaniyelik gecikme elde edilmiştir.

TABLE OF CONTENTS

LIST OF FIGURES

LIST OF TABLES

LIST OF SYMBOLS

a_k	Filter coefficient of output variables in digital filters
b_k	Filter coefficient of input variables in digital filters
$Cov(x, y)$	Covariance of x and y signals
F_s	Sampling frequency
G	Norm of 3-axis acceleration vectors in units g
G_x	X axis acceleration after sensor fusion process
G_{xb}	X axis acceleration for dorsal sensor after lowpass filtering
G_{xc}	X axis acceleration for chest sensor after lowpass filtering
G_y	Y axis acceleration after sensor fusion process
G_{yb}	Y axis acceleration for dorsal sensor after lowpass filtering
G_{yc}	Y axis acceleration for chest sensor after lowpass filtering
G_z	Z axis acceleration after sensor fusion process
G_{zb}	Z axis acceleration for dorsal sensor after lowpass filtering
G_{zc}	Z axis acceleration for chest sensor after lowpass filtering
g	Acceleration of gravity (9,80665 m/s^2)
RR	Respiration rate in cycle per minute
$RR_{Accelerometer}$	Respiration rate calculated using accelerometer sensor data
RR_{err}	Respiration rate error percentage
$RR_{Spirometer}$	Respiration rate calculated using spirometer data
T_{pa}	Peak time for accelerometer signal
T_{ps}	Peak time for spirometer signal
T'_{ps}	Previous peak time for spirometer signal
X_N	Normed form of X signal
ρ_{xy}	Correlation coefficient of x and y signals
σ_x	Standart deviation of x signal

LIST OF ACRONYMS/ABBREVIATIONS

ADC	Analog-to-Digital Converter
BLE	Bluetooth Low Energy
CCD	Charge Coupled Device
DAC	Digital-to-Analog Converter
ECG	Electrocardigram
EDR	ECG Derived Respiration
FG	Fiber Grating
FIR	Finite Impulse Response
IIR	Infinite Impulse Response
I2C	Inter Integrated Circuit
POFs	Polymeric Optical Fibres
ROI	Region of Interest
RR	Respiration Rate
RVSM	Radar Vital Signs Monitor
SAHS	Sleep Apnea/Hypopnea Syndrome
SCL	Serial Clock
SDA	Serial Data
SKLD	Symmetric Kullback-Leibler Distance
UART	Universal Asynchronous Receiver-Transmitter
USB	Universal Serial Bus
Wi-Fi	Wireless Fidelity

1. INTRODUCTION

The respiration pattern represents the volume of air in the lungs as a function of time during the respiration process. It is one of the most important vital signs that gives information about the health conditions of a person. Any disorder in the respiration pattern can be triggered by various diseases like sleep apnea, asthma, or other lung diseases [1]. There is increased research in developing respiration detection methods other than spirometry, which is the golden standard in airflow measurement. These studies aim at detecting the respiration pattern and phases without the cumbersome act of breathing into the mouthpiece of a spirometer, especially for prolonged monitoring of the body either at rest like sleep studies or in motion during exercising. This point becomes especially important with wearable monitoring systems where many parameters of the body are recorded or measured either with or without body motion. As a result, several methods to extract respiration pattern exist in literature. Some of these methods are represented in Chapter 2.

In this thesis, a method for estimating respiration pattern using two accelerometers is represented. Signal is extracted from the combination of 3-axis acceleration data. Measurements from the two sensors are fused to eliminate noise and increase the signal to noise ratio before combining the 3-axis data, making the simultaneous use of two sensors a superior approach in terms of signal amplification and noise suppression. Additionally, a 3rd order IIR filter is applied to axis-signals to further filter out noise. Relevant comparisons are introduced in Chapter 4. Delay and correlation values are used to compare the results with an ultrasonic based spirometer. Main motivation in this thesis is to design a low cost, easy to use and reliable system. Combining 2 sensor data is a new approach not found in literature and enables getting better results.

Respiration rate is calculated after the extraction of the respiration pattern. Respiration rate can be defined as the number of inhalation-exhalation-pause cycles per minute [2].

Mean value of respiration rate is 30-60/min for children, 12-18/min for adults and 12-28/min for elder people [3]. 0.5 Hz cut-off frequency is selected for the low pass filter in this study because adult subjects are used in measurement tests. Respiration rate can be calculated from the respiration pattern. Respiration rate calculation algorithm is given in Chapter 4.

This thesis contains 5 chapters. Chapter 1 is introduction and it gives motivation and objective of the thesis. Chapter 2 presents literature research about respiration pattern detection and respiration rate calculation. Chapter 3 contains setup and methodology. Hardware information and software architecture are given in this chapter. Chapter 4 provides results and comparisons. Respiration pattern is compared with ultrasonic based spirometer and respiration rate is calculated. Additionally, correlation coefficient, SKLD values and mean delays are calculated in this chapter. After these comparisons, moving body tests are applied to subjects and results are compared with spirometer. Lastly, the conclusion of the thesis is given in Chapter 5.

2. RELATED WORKS

In this chapter, brief review of the literature research is presented. In recent years, scientists and engineers have developed different techniques about detection respiration pattern and airflow estimation. These techniques have several advantages over each other like ease of use and more accurate results. The diversity of studies in this field provides advantages to patients such as early diagnosis or easier disease follow-up.

There are many different methods to extract the respiration pattern. These methods can be divided two main groups: Contact based and noncontact based methods. Radar based monitoring, optical based monitoring, and thermal based monitoring systems are examples of noncontact based methods. Acoustic based systems, airflow-based systems, electrocardiogram derived systems and chest movement detection systems are examples of contact-based methods [4].

2.1. Noncontact Based Monitoring Techniques

The first noncontact based monitoring technique is optical based monitoring systems. Aoki et al. [5] have developed non restrictive sensing system using fiber grating vision sensor. This system has been used to monitor respiration system of a sleeping person. The system consists of two parts which are FG vision sensor and a processing unit. Infrared light is spotted by FG projecting device and invisible light is captured by CCD camera of FG vision sensor. Shifting in spots shows respiration pattern in the developed system.

Radar based monitoring is another way to extract respiration pattern. Greneker [6] presented a system to detect respiration and heartbeat without any connection which is called radar vital signs monitor (RVSM). The system uses Dopler shift in signal which is radiated from Gunn device. Filters and amplifiers are applied to signal to extract heartbeat and respiration signal.

Limitation of this method was artefact which corrupted the breathing signals [4].

Another noncontact technique for respiration monitoring is thermal sensor and thermal imaging based systems. Hsu and Chow [7] have developed a non-attached type apnea monitor to detect and display respiration rate (RR). The system was used for babies and infants. Thermo sensors which are placed on mask are used to detect airflow temperature. The mask should be placed close to inftants and this is a drawback for this method.

Alkali et. al. [8] focused on facial tracking in thermal images for respiration rate monitoring in another study. In this study, thermal camera is used to detect face, and facial points of interest associated with respiration are extracted. Feature extraction and signal processing techniquess are applied to region of interest (ROI) which is specified around detected point of interests. This system tracks respiration system in real time with 40ms frame computation time.

Consequently, radar based, optical based and thermal sensor based systems are some examples of noncontact respiratory monitoring systems. These techniques usually use sensors to detect changes in patients' body caused by respiration. These methods have advantages over contact based techniques because they do not need to any connection with patients. However, they have not reached the level of maturity that can be used in clinical environments [4]. These methods are need to be improved to use in routine medical examinations. Next section presents contact based respiration monitoring methods which are used more widely.

2.2. Contact Based Monitoring Techniques

Contact based respiratory monitoring methods mostly use a sensor attached to the body. These sensors measure physical parameters which are respiratory airflow, chest movements caused by respiration, respiration sounds, gas changes of body. Additionally, ECG (electrocardiogram) is another way to extract respiration pattern.

Main contact based respiration detection approach is airflow measuring systems. Ciołek et al. [9] presented a new approach to detect SAHS (sleep apnea/hypopnea syndrome) from a single channel airflow record. (SAHS) is a sleepbreathing disorder characterized by obstructions of the upper airway. It results in blood oxygen desaturation or arousals leading to sleep fragmentation. Two nonlinear filters are used instead of one linear lowpass filter in this paper.

ECG derived respiration pattern extraction which is called EDR (ECG-Derived Respiration) is an alternative way to detect respiration pattern. Mazzanti et. al. [10] proposed a method which caluclates th EDR values from QRS area variations and obtains respiratory waveform through interpolation.

In acoustic based systems, lung sounds are tracked to extract respiration pattern and detect abnormal sounds which are indicators of pulmonary diseases. The most common and widely used tool to detect lung sounds is stethoscope which is invented in 1816 by Rene Laennec [11]. Lung sounds have recently been monitored digitally with the advancing technology. The most important advantage of the electronic stethoscopes is that frequency band is not limited. Lung sounds can be categorized two classes which are vesicular(normal) and advantitious(abnormal) sounds [12].

Another contact based respiration monitoring technique is chest and abdominal movement detection systems. There are several methods to extract respiration pattern using chest movements. These methods can be divided into two groups. The first group focuses on measuring the volume or circumference of the ribcage and abdomen [13]. Kherel et. al. [14] presented a respiratory sensing system which uses flexible polymeric optical fibres(POFs). POFs were integrated into a carrier fabric to form a wearable system. Four optical fibres which have different properties are used in the tests. Additionally, different setups of fibres are tested with different positionings. According to results, the fibre with Geniomer (Gm) 175 and cable section 0.5 mm has better performance. Additionally, bends and crossings in fibres attenuate the signals.

The second group of methods focus on chest and abdominal movements. Ertas and Gultekin [15] presented a device based on thoracic based motion tracking system with complementary filtering which detects the respiration pattern. A motion sensor which has three-axis accelerometer and three-axis gyroscope is used in this study. Data read by motion sensor is sent to computer over UART to USB converter. Rotation data is calculated from accelerometer and gyroscope values. Complementary filter is used to combine rotation values. Reason of using complementary filtering is that it is faster than Kalman filter and gives similiar results with Kalman filter. Additionally, accelerometer is used stand-alone to extract respiration pattern. Single, dual or tri-axis accelerometers are used to extract respiration pattern in literature [13].

In this study, we used 2 accelerometers to extract respiration pattern. Reason of not using non-contact based methods is that they can be easily affected by environmental conditions outside of clinic. Using accelerometer is comfortable for patients because they do not need to use any mask as airflow measuring techniques. Additionally, using accelerometer is easier than belts and straps. Diversely from literature works and as a new approach, we used 2 accelerometers to increase accuracy of results and eliminate irrelevant body movements. Detailed methodology is given in the next section.

3. SYSTEM IMPLEMENTATION AND METHODOLOGY

The overall system is composed of two main parts. First part is a software program written in MATLAB and is responsible for connecting to the embedded system, receiving data over the Bluetooth, filtering of data and displaying the graph of the filtered respiration pattern. Second part of the system is the embedded system which has 5 components which are given in section 2.1 namely, 2 MPU6050 6-axis (3-axis acceleration and 3-axis gyroscope) motion sensors, Atmega328 Microcontroller, HC-05 Bluetooth Module and Power Supply.

This chapter contains two sections. First section describes hardware parts of system and their features. Second section shows software architecture of system. Flowcharts for programs are given in this section. Additionally, respiration rate calculation algorithm and filtering methodology are be explained in section two.

3.1. System Hardware

This section gives information about the hardware in embedded system which have 2 MPU6050 6-axis (3-axis acceleration and 3-axis gyroscope) motion sensors, Atmega328 Microcontroller, HC-05 Bluetooth Module and Power Supply. Hardware block diagram of the embedded system is shown in Figure 3.1.

MPU6050 is the world's first integrated 6-axis MotionTracking device that combines a 3-axis gyroscope, 3-axis accelerometer, and a Digital Motion Processor™ (DMP) in a small 4x4x0.9mm package [16]. Sensor and pinout is shown in Figure 3.2. MPU6050 motion sensor has 16 bits-ADC and 2/4/8/16g maximum acceleration measurement options. These values indicates that accelerations with 0.000061035156g precision can be obtained if the system behaves linearly. Sensor communicates with microcontroller using I2C protocol. I2C is a serial communication protocol which is used to connect single/multiple masters single/multiple slaves.

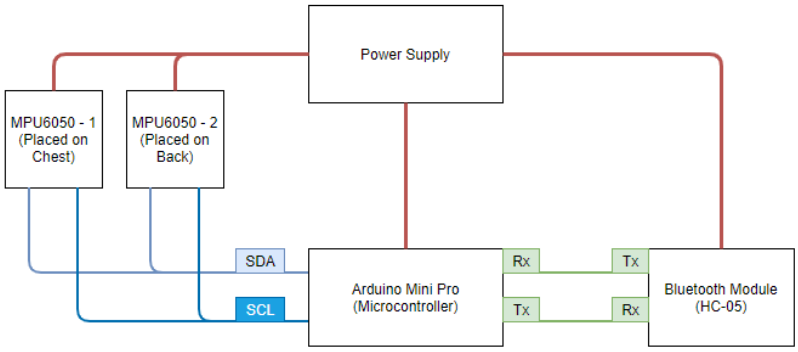

Figure 3.1. Hardware Block Diagram.

This protocol is useful for low speed DACs and ADCs, reading hardware monitors and sensors, accessing real time clocks, contolling small OLED or LCD displays etc. There are two wires in I2C communication namely SDA and SCA. SDA line is used for data transmission and SCL line is used to carry clock signal. MPU6050 sensor can be addressed with two different values using AD0 ping on board. We used 2 MPU6050 sensors in single I2C communication system using AD0 pin. Pin functions of the sensor is given in Table 3.1

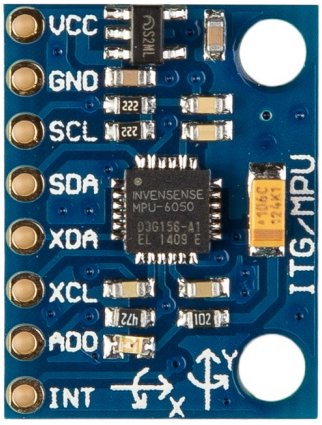

Figure 3.2. MPU6050 Sensor and Pins.

Table 3.1. MPU6050 pin functions.

Pin Name	**Description**
VCC	Power pin of sensor. Need to connect 5V to this pin.
GND	Ground pin of sensor.
SCL	Serial clock pin. Connect to microcontrollers SCL pin.
SDA	Serial Data pin. Connect to microcontrollers SDA pin.
XDA	Auxiliary Serial Data pin. It is used to connect other I2C interface enabled sensors SDA pin to MPU-6050.
XCL	Auxiliary Serial Clock pin. It is used to connect other I2C interface enabled sensors SCL pin to MPU-6050.
AD0	I2C Slave address pin.
INT	Interrupt digital output pin.

Sensor placement on the body is an important issue in order to collect accurate data. In this study, sensors were placed on the right side of the body because heart beats can affect sensors placed on the left side [17]. Heart beats have 80mg vibration while respiratory signal is about 10mg according to literature [18]. Two sensors were placed on the chest and at back of the body as axisymmetrical. Acceleration value obtained from these sensors is amplified with this method because sensors are moved in opposite directions during respiration. Additionally, undesired body movements are eliminated by combining sensor values. Sensor placement is shown in Figure 3.3.

HC-05 module is used as the communication device in this study. HC-05 module is an easy to use Bluetooth SPP (Serial Port Protocol) module, designed for transparent wireless serial connection setup [19]. It has -80dBm sensitivity and supports master and slave modes. Figure 3.4 shows HC-05 module illustration and Table 3.2 explains pin functions of module.

HC-05 module supports different baud rates options from 9600 to 115200. Baud rate refers to the number of bits transmitted per second.

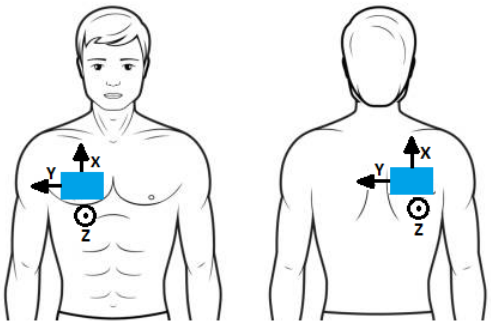

Figure 3.3. Sensor Placement on Body.

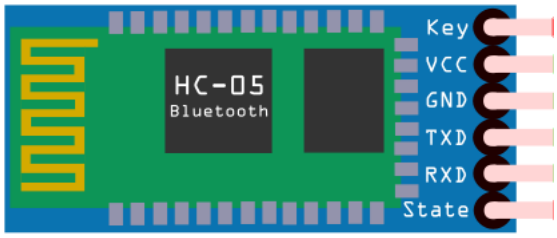

Figure 3.4. HC-05 Bluetooth Module Illustration.

Table 3.2. HC-05 Pin Functions.

Pin Name	**Description**
Key	Enable pin. It is used to bring the module in AT commands mode.
VCC	Power pin of module. Need to connect 5V or 3.3V to this pin. Board has internal 3.3V regulator.
GND	Ground pin of module.
TXD	Transmit pin. Connect receive pin of microcontroller.
RXD	Receive pin. Connect transmit pin of microcontroller.
State	It is used to check if module is connected.

In this study, 115200 baud rate is used because lower baud rates cause timing problems. The message which is sent from microcontroller is 32 bytes and its structure is given in the next section. The message is sent in 26.6 milliseconds at 9600 baud rate and in 2.2 milliseconds at 115200 baud rate. Byte time according to baud rate can be derived as

$$\text{ByteTimeInSecond} = \frac{8}{\text{BaudRate}}. \tag{3.1}$$

HC-05 module is used as the server. Another application is written in C language to configure bluetooth module. AT commands are used to configure HC-05. List of the used AT commands is given in Table A.1.

The Arduino Pro Mini microcontroller board is used in this project. It is based on ATmega328 microchip, designed and manufactured by SparkFun Electronics [20]. Arduino Pro Mini has 14 digital input/output pins, 6 analog inputs. 32KB flash memory 16 MHz Clock speed. It supports I2C, serial and SPI communication protocols. Main reasons of selecting this microcontroller are having few but sufficient digital pins, supporting required communication protocols and small dimensions (1.778cm x 3.302cm). Schematic of microcontroller is given in Figure 3.5. In our study, personal computer is used as a power supply.

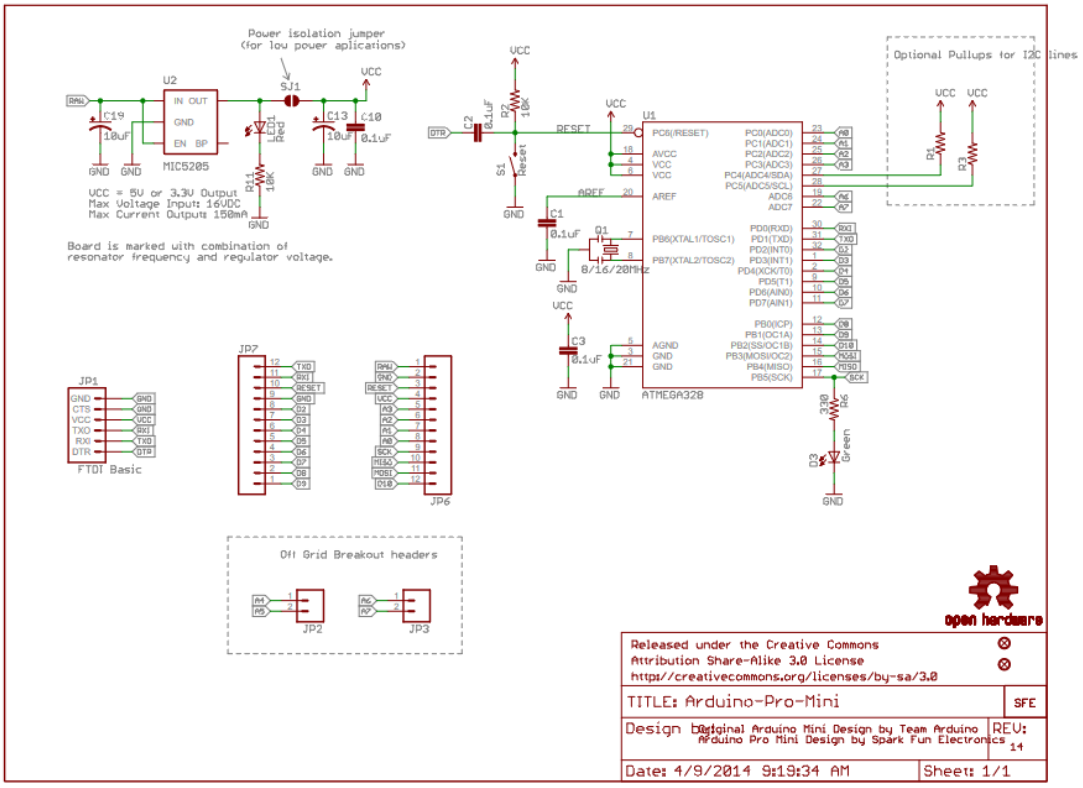

Figure 3.5. Arduino Pro Mini Schematic.

3.2. System Software and Algorithms

The overall system is composed of two main software programs. First program is an embedded software that runs on microcontroller. Code flowchart is given in Figure 3.6.

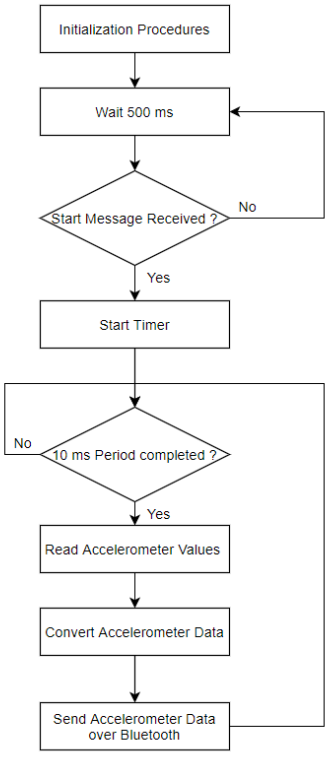

Figure 3.6. Flowchart of Microcontroller.

In initialization state, baud rate of bluetooth series channel is set to 115200 and MPU sensors are intialized first. Full scale acceleration range is set 2 for both sensors. After these steps, bluetooth module is reset with "AT+RESET" command and wait connections. System waits "START" message to start main flow at this stage. Operation time is checked periodically in main loop with standart micros() functions. MPU6050 acceleration values are read when 10 ms period is completed. Read values are divided to 16384.0 to transform to g value. Transformed values are sent to MATLAB application with 32-byte message. Message structure is given in Table 3.3. Reserved values are used for timing tests.

Table 3.3. Message Structure.

Parameter Name	**Parameter Size**	**Description**
Acc_X_Chest	4 Byte(uint)	Acc Value of X Axis For Chest Sensor
Acc_Y_Chest	4 Byte(uint)	Acc Value of Y Axis For Chest Sensor
Acc_Z_Chest	4 Byte(uint)	Acc Value of Z Axis For Chest Sensor
Acc_X_Back	4 Byte(uint)	Acc Value of X Axis For Dorsal Sensor
Acc_Y_Back	4 Byte(uint)	Acc Value of Y Axis For Dorsal Sensor
Acc_Z_Back	4 Byte(uint)	Acc Value of Z Axis For Dorsal Sensor
Reserved_1	4 Byte(uint)	Reserved Value 1
Reserved_2	4 Byte(uint)	Reserved Value 2

Bluetooth module is configured using AT commands. Another arduino application which is given in Table A.1 is written to configure bluetooth module. Bluetooth name, password and baud rate are adjusted with this application.

Second software program is written in MATLAB and is responsible for connecting to the embedded system, receiving data over the Bluetooth, filtering of data and displaying the graph of filtered respiration pattern. User Interface of the MATLAB program is shown in Figure 3.8. Bluetooth connection is created with "Connect Device" button. Start button sends a message to the microcontroller to start its timer to collect accelerometer data. Figure 3.8 shows procedures after receiving data. Data is received with 0.001 precision over bluetooth. This application is started to be used after filtering and fusion techniques reached a certain level of maturity. Filtering tests, sensor fusion tests and comparisons with spirometer were done with another test script. Raw data of 2 sensors is saved using "Save" button.

Accelerometers have 0.000061035156g precision and they can be easily affected by noise. Figure 3.9 shows raw data for 3-axis obtained by sensors. We need to apply lowpass filter to eliminate noise before any sensor or axis fusion process. Digital filters can be divided to 2 main groups which are IIR and FIR filters.

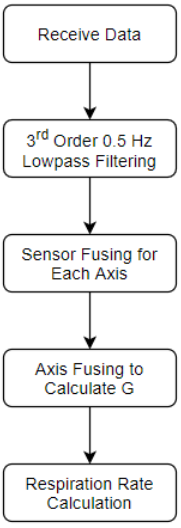

Figure 3.7. Flowchart of MATLAB Application.

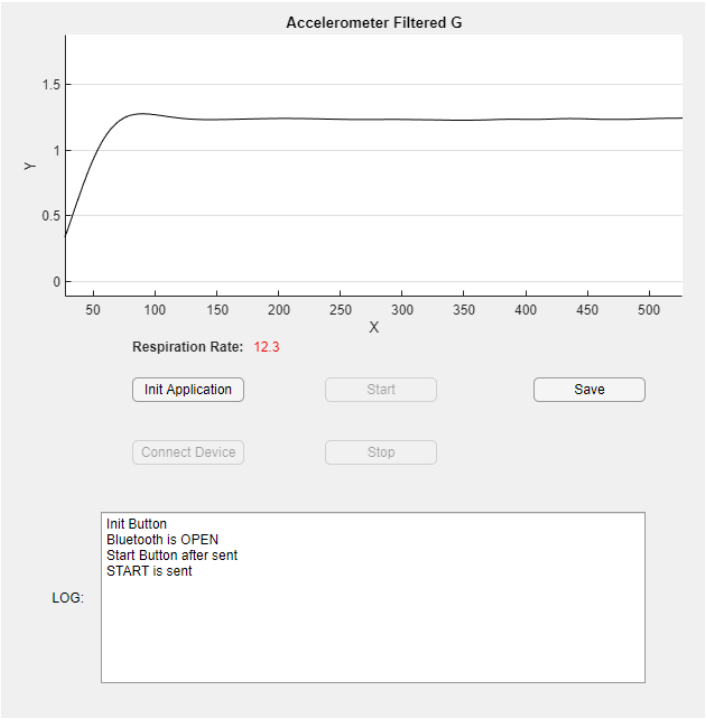

Figure 3.8. MATLAB Application User Interface.

FIR filters generates a finite impulse response of a dynamic system. Generalized formula of FIR filters can be shown as

$$\mathbf{y(n)} = \sum_{k=0}^{q} \mathbf{b_k x(n-k)}. \tag{3.2}$$

IIR filters are designed to generate infinite impulse response of a dynamic system. IIR filters have an internal feedback mechanism which means past output samples effect the result. Nature of IIR filters is recursive. Generalized formula of IIR filter can be shown as

$$\mathbf{y(n)} = \sum_{k=0}^{q} \mathbf{b_k x(n-k)} - \sum_{k=1}^{p} \mathbf{a_k y(n-k)}. \tag{3.3}$$

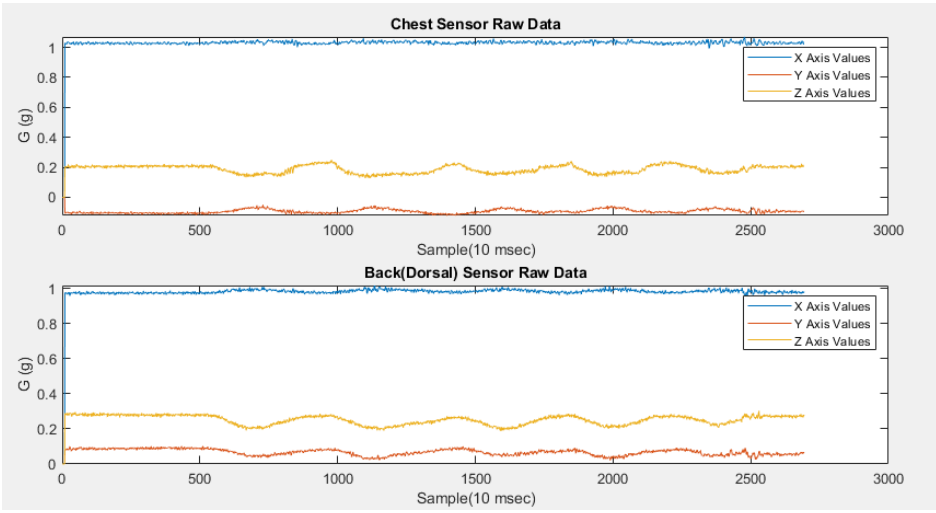

Figure 3.9. Sensor Raw Data.

Figure 3.10 shows a comparison between 3rd order lowpass butterworth IIR and 50th order low pass window-hamming FIR filter applied on the same signal. IIR and FIR filter coefficients are calculated MATLAB filterDesigner tool. filterDesigner tool is shown in Figure 3.11. According to comparisons, IIR filter has smoother results.

Additionally lowpass Butterworth filter has fewer calculations and fewer storage for coefficients because of low order. In the next steps of this study, 3rd order 0.5 Hz cutoff frequency IIR Butterworth filter is used because of these reasons. 0.5 Hz cutoff frequency is selected because mean value of respiration rate is 12-18/min for adults.

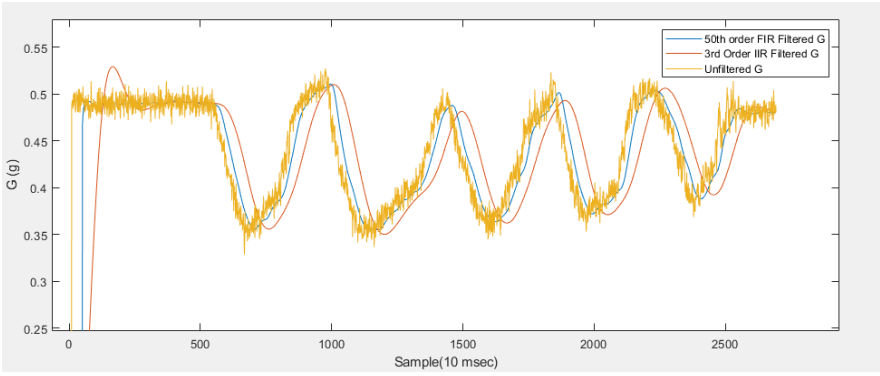

Figure 3.10. IIR and FIR Filter Comparison.

Sensor fusion process is applied for each axis after low pass filtering. In sensor fusion process, X axis values of sensors are subtracted from each other since they represent the same direction on body. Z and Y axis values are summed because they represent opposite directions according to Figure 3.3. G_x, G_y and G_z axis acceleration values after sensor combination can be derived as

$$\begin{aligned} \mathbf{G_x} &= \mathbf{G_{xc}} - \mathbf{G_{xb}} \\ \mathbf{G_y} &= \mathbf{G_{yc}} - \mathbf{G_{yb}} \\ \mathbf{G_z} &= \mathbf{G_{zc}} - \mathbf{G_{zb}}. \end{aligned} \tag{3.4}$$

G value which is the norm of 3-axis acceleration vector is calculated after sensor fusion. G can be calculated as

$$\mathbf{G} = \sqrt{\mathbf{G_x^2} + \mathbf{G_y^2} + \mathbf{G_z^2}}. \tag{3.5}$$

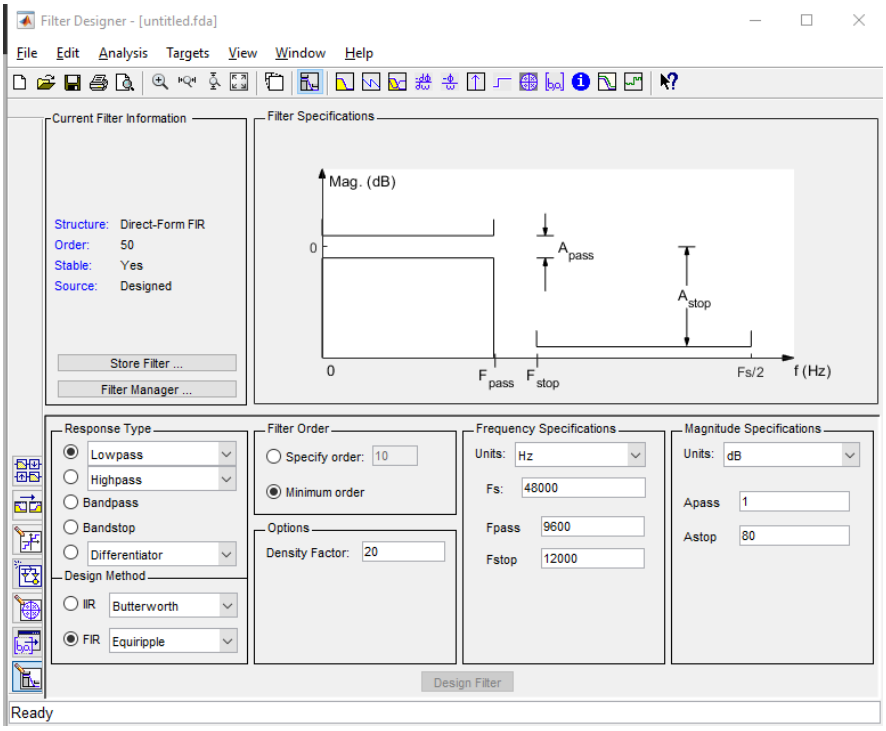

Figure 3.11. MATLAB filterDesigner Tool.

G_x, G_y and G_z show axis acceleration values after sensor combination. G_{xc}, G_{yc} and G_{zc} show chest sensor axis acceleration after lowpass filtering. G_{xb}, G_{yb} and G_{zb} show back (dorsal) sensor axis acceleration after lowpass filtering. Combining two sensors has two main advantages for the implemented system. The first advantage is amplifying the output signal. Figure 3.12 shows G values of each sensor and combined G value after sensor fusing. Peak-Valley difference increased from 0.01g to 0.15g after sensor fusing. The second advantage is eliminating effects of unwanted body movements.

Verification of respiration pattern is required after calculating G. Ultrasonic based spirometer is used as reference standart for comparisons. Spirometer measures flow rate in ml/sec and sends measured values to computer or mobile phone using BLE protocol. Sampling rate of spirometer is 200 Hz. Volume change is calculated from flow rate using spirometer. G values and volume change are normalized to make a meaningful respiration pattern comparison because they are measured with different units.

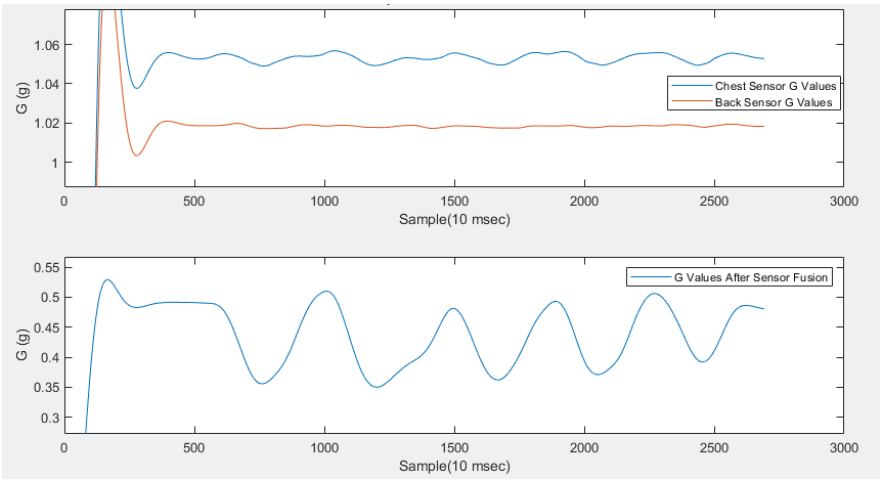

Figure 3.12. G Values of Each Sensor and G Value After Sensor Combination.

Figure 3.13 shows a comparison between volume change calculated with spirometer and respiration pattern using G values. Peak points in graphs show inhalation starting points because spirometer measures negative values during inhalation. Detailed comparisons between these two signals are made in Chapter 4.

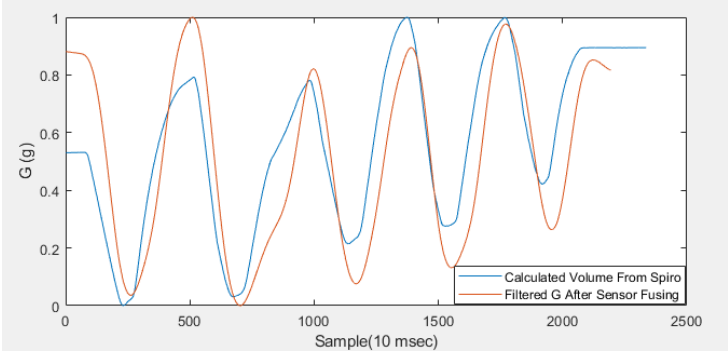

Figure 3.13. Spirometer Volume vs Filtered G After Sensor Fusion.

Second step in this study is to calculate respiration rate using respiration pattern. We have focused on calculating respiration rate after similarity between spirometer and accelerometer signals was reached. Respiration rate can be calculated as

$$\mathrm{RR} = \frac{\mathrm{Fs} \ * 60}{\mathrm{PeaktoPeakSampleCount}}. \tag{3.6}$$

Fs is sampling frequency. RR represents the number of complete inhalation and exhalation cycles in a minute. Peaks and valleys are found to calculate peak to peak sample count. Figure 3.14 shows algorithm which is used to find peak and valley points. This algorithm is originated from a study which is presented by Preejith et. al. [1]. Algorithm finds valley values in addition to peak values despite the fact that they are not used in RR calculation algorithm. Finding valleys helps to eliminate fake peaks using different thresholds.

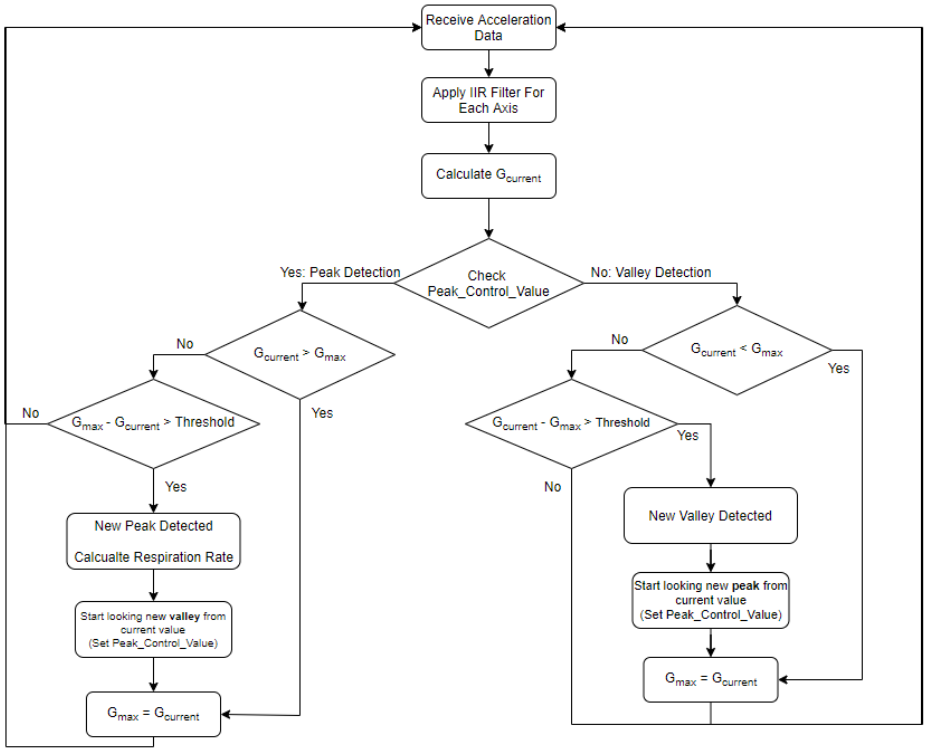

Figure 3.14. Respiration Rate Calculation Flowchart.

4. RESULTS AND COMPARISONS

This chapter presents a detailed comparison between accelerometer signal and spirometer signal in order to validate and evaluate the implemented system. Figure4.1 shows ultrasonic based spirometer used in tests. Comparisons are made by three different perspectives. Firstly, spirometer and accelerometer signals are given on the same figure and later peak to peak and mean delays are calculated. Secondly, correlation coefficients between two signals are calculated for the whole window and peak to peak sections. Coefficient correlation method is used to calculate the correlation between the two signals [21].

Figure 4.1. Ultrasonic Based Spirometer.

Correlation coefficient of two signals can be derived as

$$\rho_{xy} = \frac{\text{Cov(x,y)}}{\sigma_x * \sigma_y} \tag{4.1}$$

where ρ_{xy} is correlation coefficient of x and y signals. Cov(x,y) means covariance of x and y. σ_{x} and σ_{y} show standart deviations of signals. After finding correlation coefficients, SKLD is calculated for two signals.

SKLD (Simetric Kullback Leibler Distance) compares the likeness of two functions [22]. SKLD for two signals can be derived as

$$\text{SKLD} = \sum_{k=1}^{N} X_n(k) * ln(\frac{X_n(k)}{Y_n(k)}) + \sum_{k=1}^{N} Y_n(k) * ln(\frac{Y_n(k)}{X_n(k)}) \tag{4.2}$$

where X_n and Y_n are normed forms of X and Y signals. N means length of signal. Normed form of a signal can be calculated as

$$X_n = \frac{X}{\text{Sum(X)}}. \tag{4.3}$$

MATLAB User interface application is used to show respiration pattern signal and extract respiration rate. Another MATLAB program is used for comparisons between accelerometer and spirometer signals. Algorithm of second MATLAB program which is used for comparisons is given in Figure 4. Spirometer logs measured values in big-endian format and MATLAB application in my computer uses values in little-endian format. Therefore we need to byte swapping in spirometer data to use in the correct way.

This chapter contains two sections which are divided according to test scenarios. Scenario 1 includes tests with stable body and Scenario 2 includes tests with moving body. Test details and results are given in related sections.

4.1. Scenario 1: Tests With Stable Body

Scenario 1 tests are carried out while body was standing still. Duration of tests are between 26.1 and 39.9 seconds. Minimum five cycles data are collected for each test. In the following parts, graphical comparisons, respiration peak and valley delays, respiration rate errors and correlation coefficients between sensor fused filtered G and calculated spirometer volume are introduced.

Require: Chest X,Y,Z Data, Dorsal X,Y,Z data and Spirometer Data

Byte swapping for Spirometer data using **swapbytes** function;

Compute the mean $\mathbf{a_k}$ and $\mathbf{b_k}$ values using **butter** function;

for $k = 1$ to $Length(AccelerometerData)$ **do**

  Apply low pass filter for each Accelerometer data using Eq3.3;

  Combine sensor values for each axis and calcualte $\mathbf{G_x}$, $\mathbf{G_y}$ and $\mathbf{G_z}$ values;

  Combine axis values and calculate $\mathbf{G}$ using Eq3.5;

end for

Normalize G data and Accelerometer Data;

Plot normalized G and Accelerometer Data;

Calculate respiration rate using algorithm given in Figure3.14;

Calculate correlation coefficient using Eq4.1;

Calculate SKLD using Eq4.2;

Figure 4.2. MATLAB Comparison Program Algorithm.

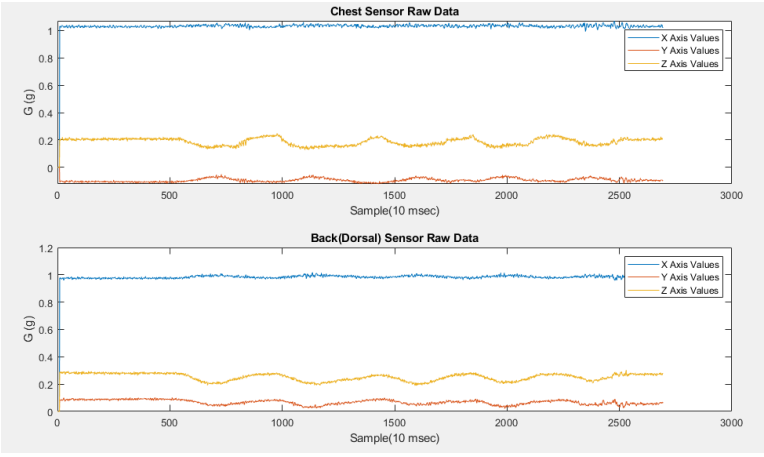

Figure 4.3. Raw Data of Back (Dorsal) and Chest Sensor for Test 1.

Figure 4.3 shows raw data of dorsal and chest sensors. There is a significant amount of noise in all axis data before filtering. After applying IIR filter for each axis, G value is calculated for both chest and dorsal sensors to see the effect of axis fusing process. Sensor fusing proess amplifies G value approximately 10-15 times as it seen in figure 4.4. This amplification is helpful in calculating respiration rate and tracking respiration pattern.

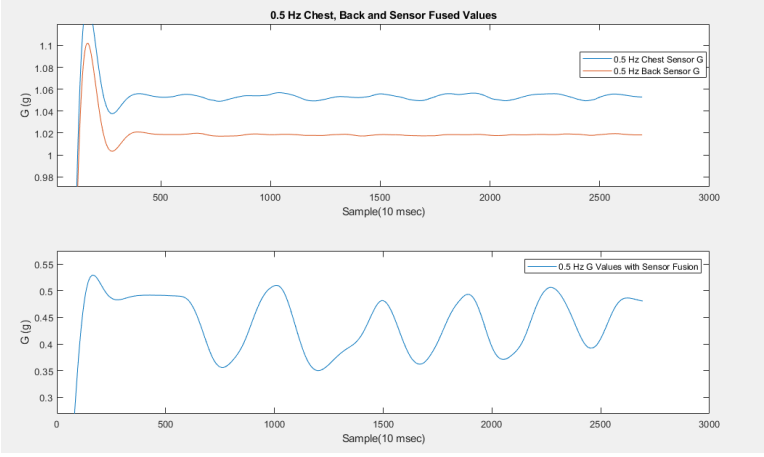

Figure 4.4. Comparison Between Sensor G values and Fused G values.

Figure 4.5 shows comparison between spirometer volume and sensor fused G. Y axis shows normalized values because two data sets are in different units. Table 4.1 shows delays for each peak/valley dealys and mean values between two data. Table 4.2 shows respiration rates for two data, respiration rate errors and correlation coefficients for each respiration cycle. Unit of $\mathrm{RR_{Accelometer}}$ and $\mathrm{RR_{Spirometer}}$ columns is cycle per minutes. Respiration rate error can be calculated as

$$RR_{err} = \frac{|RR_{Accelerometer} - RR_{Spirometer}|}{RR_{Spirometer}} * 100. \tag{4.4}$$

In the following parts of this section, other test results are given. In total, results of five tests are presented in this scenario.

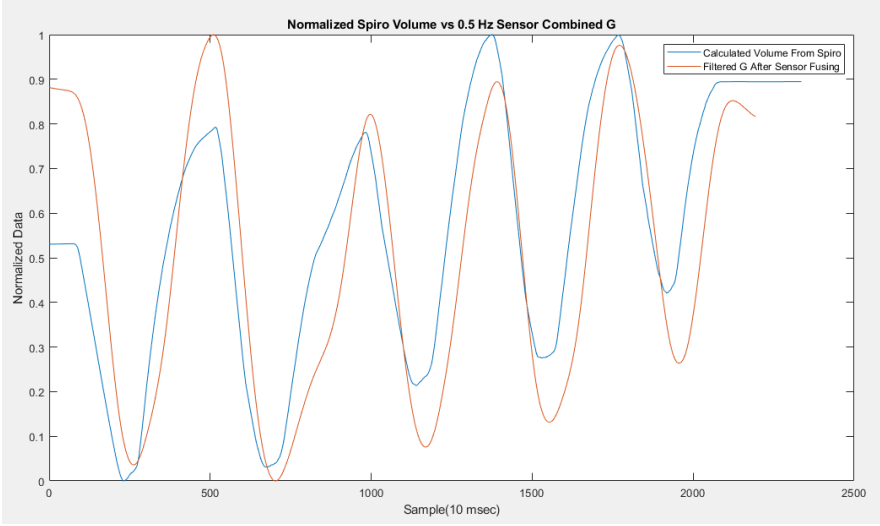

Figure 4.5. Comparison Between Sensor G Values And Fused G Values (Test 1).

Table 4.1. Scenario 1 Test 1 Peak and Valley Delays.

Cycles	**Peak to Peak Delay (ms)**	**Valley to Valley Delay (ms)**
Cycle 1	-730 ms	310 ms
Cycle 2	-60 ms	310 ms
Cycle 3	150 ms	290 ms
Cycle 4	160 ms	240 ms
Cycle 5	30 ms	370 ms
Mean	226 ms	304 ms

Table 4.2. Scenario 1 Test 1 Respiration Rates and Correlation Coefficients.

Cycles	$\mathbf{RR_{Accelerometer}}$	$\mathbf{RR_{Spirometer}}$	**RR Error**	**Correlation Coef**
Cycle 1-2	13.57 Cycle/min	11.78 Cycle/min	15.20 %	0.8222
Cycle 2-3	12.87 Cycle/min	12.32 Cycle/min	4.46 %	0.8167
Cycle 3-4	15.26 Cycle/min	15.22 Cycle/min	0.26 %	0.8610
Cycle 4-5	15.27 Cycle/min	15.79 Cycle/min	3.29 %	0.9071
Mean	14.36 Cycle/min	13.77 Cycle/min	4.10 %	0.7964 (All Data)

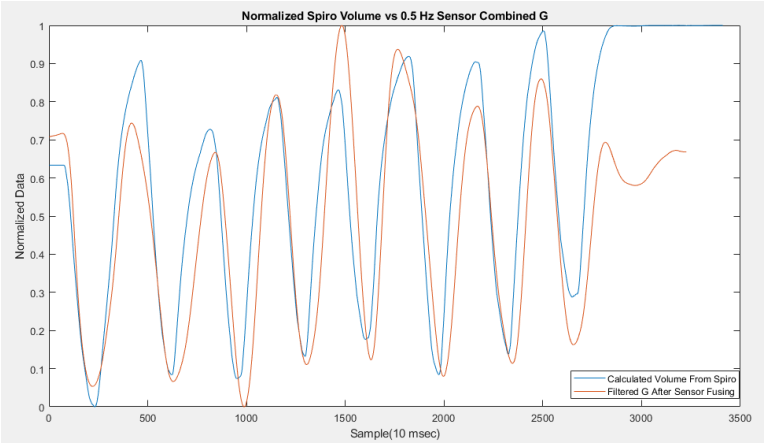

Figure 4.6. Comparison Between Sensor G Values And Fused G Values (Test 2).

Table 4.3. Scenario 1 Test 2 Peak and Valley Delays.

Cycles	**Peak to Peak Delay (ms)**	**Valley to Valley Delay (ms)**
Cycle 1	660 ms	-110 ms
Cycle 2	-470 ms	60 ms
Cycle 3	270 ms	370 ms
Cycle 4	-40 ms	70 ms
Cycle 5	180 ms	270 ms
Cycle 6	-570 ms	220 ms
Cycle 7	110 ms	210 ms
Cycle 8	-120 ms	50 ms
Mean	302 ms	170 ms

Table 4.4. Scenario 1 Test 2 Respiration Rates and Correlation Coefficient.

Cycles	**$RR_{Accelerometer}$**	**$RR_{Spirometer}$**	**RR Error**	**Correlation Coef.**
Cycle 1-2	12.90 Cycle/min	17.04 Cycle/min	24.30 %	0.9506
Cycle 2-3	17.19 Cycle/min	14.18 Cycle/min	21.19 %	0.9182
Cycle 3-4	17.70 Cycle/min	19.48 Cycle/min	9.14 %	0.8169
Cycle 4-5	19.35 Cycle/min	18.07 Cycle/min	7.08 %	0.8952
Cycle 5-6	16.78 Cycle/min	21.20 Cycle/min	20.85 %	0.7864
Cycle 6-7	17.35 Cycle/min	14.85 Cycle/min	20.20 %	0.8584
Cycle 7-8	17.39 Cycle/min	18.63 Cycle/min	6.66 %	0.8962
Mean	17.02 Cycle/min	17.63 Cycle/min	3.46 %	0.8210 (All Data)

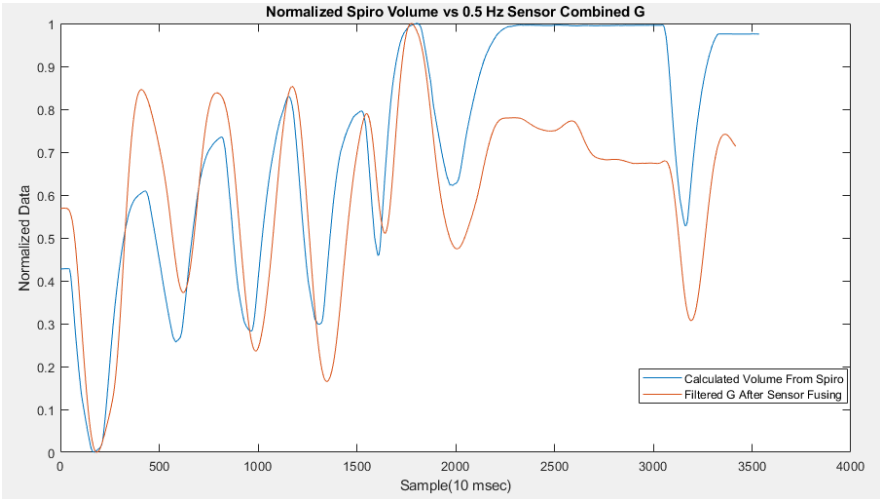

Figure 4.7. Comparison Between Sensor G Values And Fused G Values (Test 3).

Table 4.5. Scenario 1 Test 3 Peak and Valley Delays.

Cycles	**Peak to Peak Delay (ms)**	**Valley to Valley Delay (ms)**
Cycle 1	-140 ms	110 ms
Cycle 2	-180 ms	370 ms
Cycle 3	-240 ms	210 ms
Cycle 4	190 ms	380 ms
Cycle 5	260 ms	330 ms
Cycle 6	-290 ms	230 ms
Cycle 7	-2220 ms	280 ms
Mean	502 ms	272 ms

Table 4.6. Scenario 1 Test 3 Respiration Rates and Correlation Coefficient.

Cycles	$\mathbf{RR_{Accelerometer}}$	$\mathbf{RR_{Spirometer}}$	**RR Error**	**Correlation Coef.**
Cycle 1-2	15.50 Cycle/min	15.34 Cycle/min	1.04 %	0.8991
Cycle 2-3	15.75 Cycle/min	15.50 Cycle/min	1.61 %	0.7747
Cycle 3-4	15.66 Cycle/min	17.64 Cycle/min	11.22 %	0.7733
Cycle 4-5	15.96 Cycle/min	16.26 Cycle/min	1.85 %	0.6396
Cycle 5-6	26.43 Cycle/min	21.28 Cycle/min	24.20 %	0.7257
Cycle 6-7	11.53 Cycle/min	8.42 Cycle/min	36.94 %	0.8628
Mean	16.81 Cycle/min	15.74 Cycle/min	6.36 %	0.7478 (All Data)

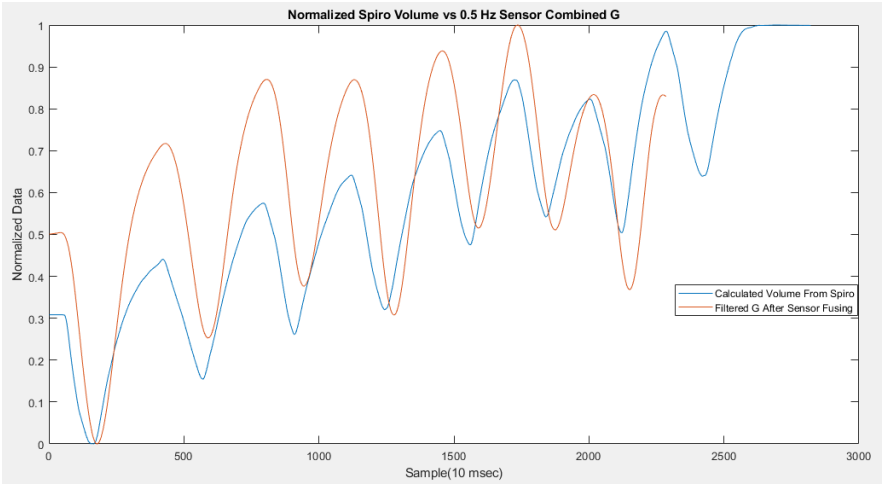

Figure 4.8. Comparison Between Sensor G Values And Fused G Values (Test 4).

Table 4.7. Scenario 1 Test 4 Peak and Valley Delays.

Cycles	**Peak to Peak Delay (ms)**	**Valley to Valley Delay (ms)**
Cycle 1	40 ms	140 ms
Cycle 2	100 ms	200 ms
Cycle 3	120 ms	350 ms
Cycle 4	110 ms	350 ms
Cycle 5	100 ms	310 ms
Cycle 6	90 ms	330 ms
Cycle 7	150 ms	290 ms
Mean	102 ms	281 ms

Table 4.8. Scenario 1 Test 4 Respiration Rates and Correlation Coefficient.

Cycles	**$RR_{Accelerometer}$**	**$RR_{Spirometer}$**	**RR Error**	**Correlation Coef.**
Cycle 1-2	15.42 Cycle/min	15.83 Cycle/min	2.59 %	0.9440
Cycle 2-3	16.00 Cycle/min	16.09 Cycle/min	0.56 %	0.9175
Cycle 3-4	18.52 Cycle/min	18.46 Cycle/min	0.33 %	0.7546
Cycle 4-5	18.41 Cycle/min	18.35 Cycle/min	0.33 %	0.7677
Cycle 5-6	21.58 Cycle/min	21.50 Cycle/min	0.37 %	0.6869
Cycle 6-7	21.20 Cycle/min	21.66 Cycle/min	2.12 %	0.6808
Mean	18.52 Cycle/min	18.64 Cycle/min	0.65 %	0.7757 (All Data)

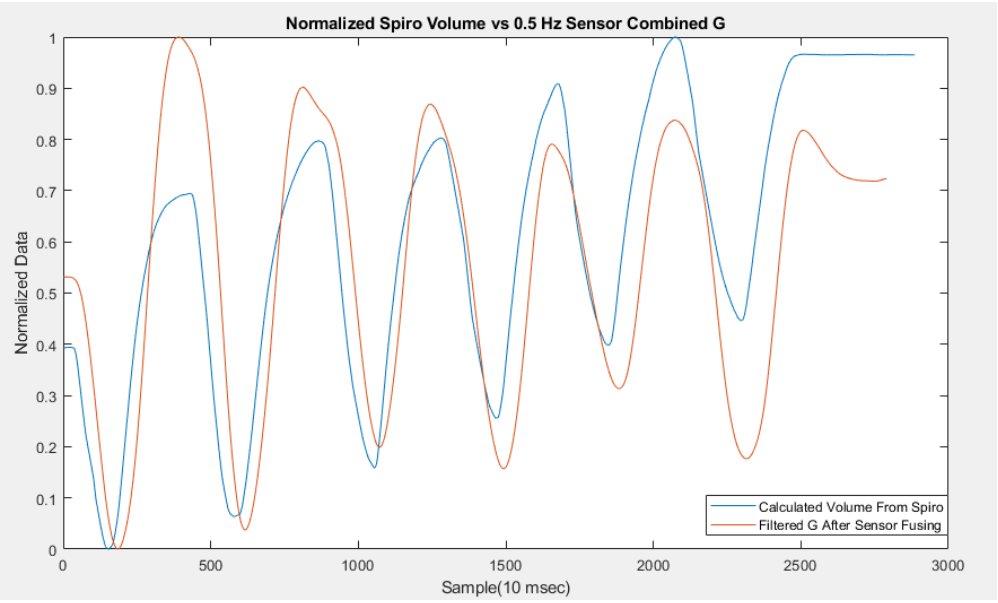

Figure 4.9. Comparison Between Sensor G Values And Fused G Values (Test 5).

Table 4.9. Scenario 1 Test 5 Peak and Valley Delays.

Cycles	**Peak to Peak Delay (ms)**	**Valley to Valley Delay (ms)**
Cycle 1	190 ms	620 ms
Cycle 2	-100 ms	660 ms
Cycle 3	-240 ms	470 ms
Cycle 4	80 ms	570 ms
Cycle 5	100 ms	670 ms
Cycle 6	290 ms	470 ms
Mean	166 ms	576 ms

Table 4.10. Scenario 1 Test 5 Respiration Rates and Correlation Coefficients.

Cycles	$\mathbf{RR_{Accelerometer}}$	$\mathbf{RR_{Spirometer}}$	**RR Error**	**Correlation Coef**
Cycle 1-2	15.75 Cycle/min	14.63 Cycle/min	7.66 %	0.8542
Cycle 2-3	14.25 Cycle/min	13.79 Cycle/min	3.34 %	0.8119
Cycle 3-4	13.89 Cycle/min	14.42 Cycle/min	3.68 %	0.8774
Cycle 4-5	14.56 Cycle/min	15.22 Cycle/min	4.34 %	0.8555
Cycle 5-6	14.39 Cycle/min	15.07 Cycle/min	4.51 %	0.8310
Mean	14.56 Cycle/min	14.62 Cycle/min	0.42 %	0.7522 (All Data)

According to scenario 1 results, implemented system has 100% accuracy in detecting peak and valley points. There are some differences between peak and valley points of spirometer and accelerometer data. Averages of 260 msec peak to peak delay and 321 msec valley to valley delay are calculated according to results. Greater valley to valley delay is not important to us because only peak values are used to calculate respiration rate. 'Respiration Rates and Correlation Coefficients' tables show calculated respiration rate values for each cycle. 8.54% avarage error is estimated when each cycle is considered one by one. 2.99% avarage error is calculated when each test is considered as a whole window. These values show averaging a given number of samples will give better results than using only last peak to peak value. Correlation coefficient is calculated as 0.8280 when data is taken as peak to peak windows for all scenario 1 tests. 0.7786 is correlation coefficient when data is taken as whole window for each test.

4.2. Scenario 2: Tests With Moving Body

In this section, tests are performed while body is moving. Data is collected for a minimum of four respiration cycles for each test. Random motions are realised in the first 3 tests. Test 4 shows results while periodic reciprocating motions going. Test 5 shows results of rotational movements. In the following parts, scenario 2 test results and comparisons are given.

Table 4.11. Scenario 2 Test 1 Peak and Valley Delays.

Cycles	**Peak to Peak Delay (ms)**	**Valley to Valley Delay (ms)**
Cycle 1	60 ms	720 ms
Cycle 2	460 ms	990 ms
Cycle 3	-280 ms	570 ms
Cycle 4	820 ms	630 ms
Mean	405 ms	725 ms

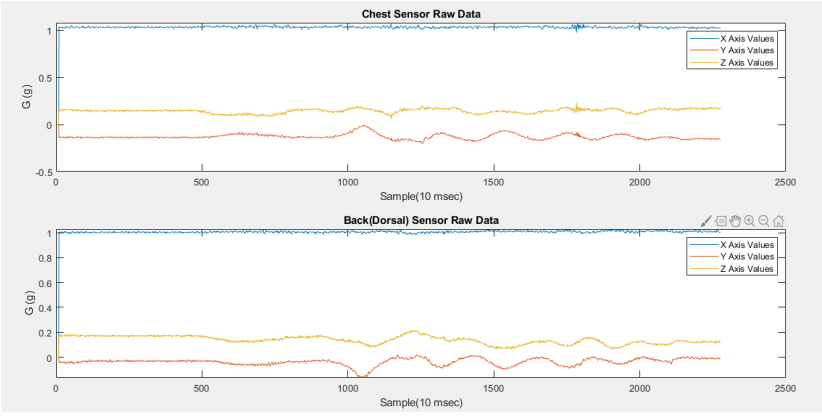

Figure 4.10. Raw Data of Back (Dorsal) and Chest Sensor for Test 1.

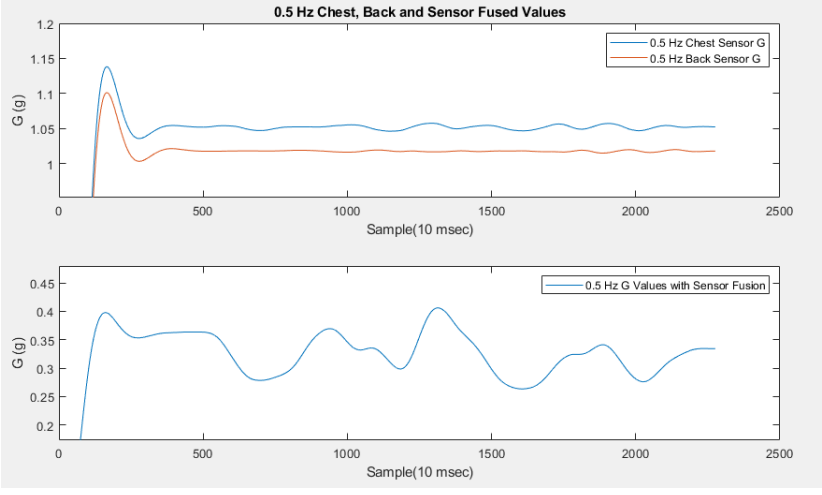

Figure 4.11. Comparison Between Sensor G Values and Fused G Values for Test 1.

Table 4.12. Scenario 2 Test 1 Respiration Rates and Correlation Coefficients.

Cycles	**$RR_{Accelerometer}$**	**$RR_{Spirometer}$**	**RR Error**	**Correlation Coef.**
Cycle 1-2	13.66 Cycle/min	15.04 Cycle/min	9.16 %	0.8576
Cycle 2-3	16.00 Cycle/min	13.36 Cycle/min	19.76 %	0.8431
Cycle 3-4	10.51 Cycle/min	13.01 Cycle/min	19.22 %	0.8666
Mean	13.39 Cycle/min	13.80 Cycle/min	3.07 %	0.6239 (All Data)

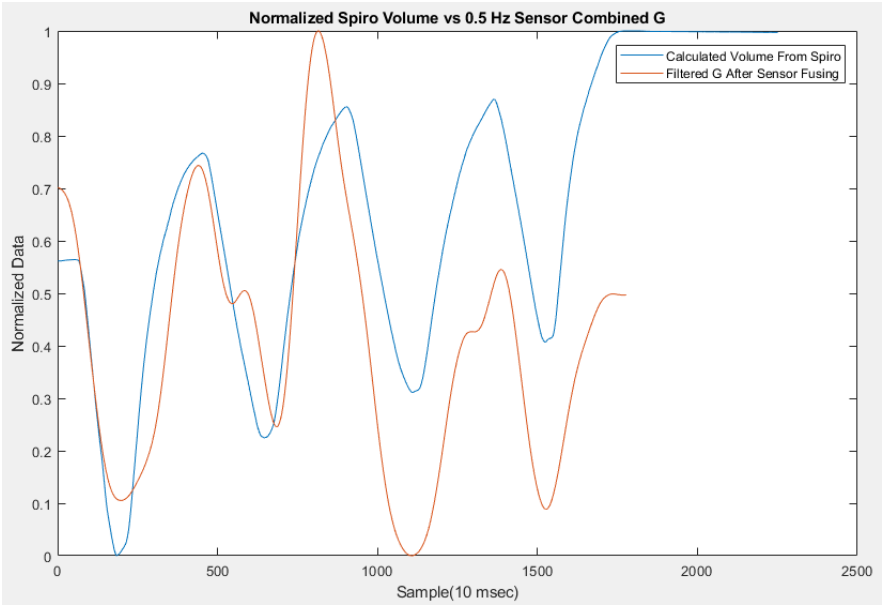

Figure 4.12. Comparison Between Sensor G Values And Fused G Values (Test 1).

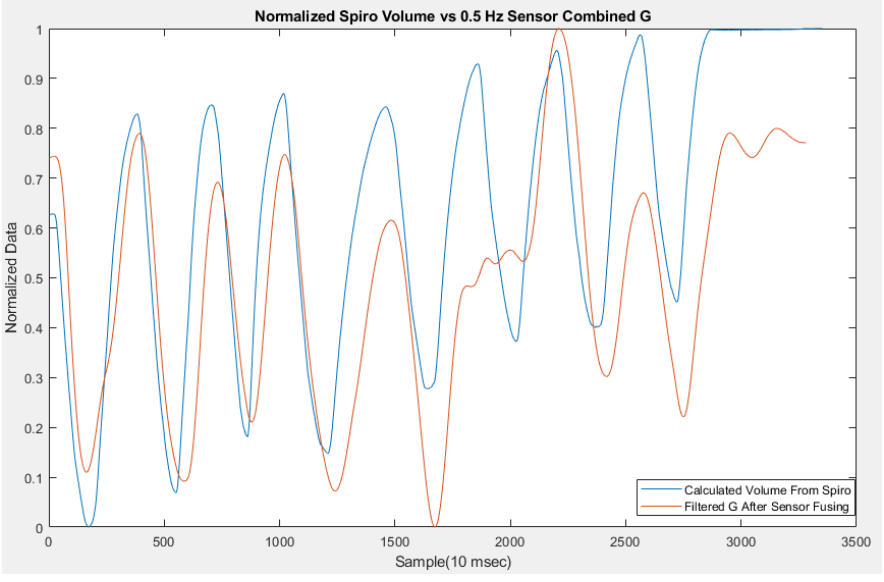

Figure 4.13. Comparison Between Sensor G Values And Fused G Values (Test 2).

Table 4.13. Scenario 2 Test 2 Peak and Valley Delays.

Cycles	**Peak to Peak Delay (ms)**	**Valley to Valley Delay (ms)**
Cycle 1	100 ms	-100 ms
Cycle 2	100 ms	350 ms
Cycle 3	270 ms	190 ms
Cycle 4	40 ms	300 ms
Cycle 5	230 ms	290 ms
Cycle 6	3520 ms	3910 ms
Cycle 7	3760 ms	3820 ms
Cycle 8	Not Detect	Not Detect
Mean	1140 ms	1280 ms

Table 4.14. Scenario 2 Test 2 Respiration Rates and Correlation Coefficients.

Cycles	$\mathbf{RR_{Accelerometer}}$	$\mathbf{RR_{Spirometer}}$	**RR Error**	**Correlation Coef.**
Cycle 1-2	16.30 Cycle/min	16.31 Cycle/min	0.06 %	0.8956
Cycle 2-3	17.70 Cycle/min	18.63 Cycle/min	4.99 %	0.6720
Cycle 3-4	20.62 Cycle/min	19.11 Cycle/min	7.90 %	0.8186
Cycle 4-5	13.01 Cycle/min	13.58 Cycle/min	4.20 %	0.7481
Cycle 5-6	8.24 Cycle/min	15.04 Cycle/min	45.21 %	0.8076
Cycle 6-7	16.39 Cycle/min	17.54 Cycle/min	6.56 %	0.6646
Cycle 7-8	Not Detect	16.57 Cycle/min	100.0 %	0.4779
Mean	15.37 Cycle/min	16.68 Cycle/min	7.85 %	0.7519 (All Data)

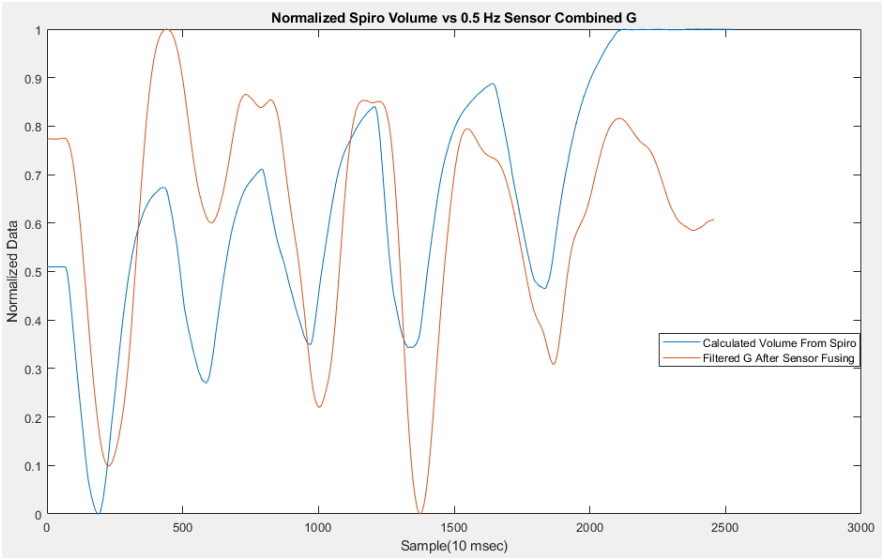

Figure 4.14. Comparison Between Sensor G Values And Fused G Values (Test 3).

Table 4.15. Scenario 2 Test 3 Peak and Valley Delays.

Cycles	**Peak to Peak Delay (ms)**	**Valley to Valley Delay (ms)**
Cycle 1	200 ms	580 ms
Cycle 2	360 ms	400 ms
Cycle 3	-400 ms	540 ms
Cycle 4	-190 ms	640 ms
Cycle 5	-720 ms	530 ms
Mean	374 ms	538 ms

Table 4.16. Scenario 2 Test 3 Respiration Rates and Correlation Coefficients.

Cycles	**$RR_{Accelerometer}$**	**$RR_{Spirometer}$**	**RR Error**	**Correlation Coef.**
Cycle 1-2	15.78 Cycle/min	16.48 Cycle/min	4.25 %	0.7703
Cycle 2-3	20.62 Cycle/min	16.35 Cycle/min	26.12 %	0.7332
Cycle 3-4	13.79 Cycle/min	14.49 Cycle/min	4.83 %	0.6229
Cycle 4-5	15.71 Cycle/min	13.79 Cycle/min	13.92 %	0.7384
Mean	16.47 Cycle/min	15.27 Cycle/min	7.85 %	0.5058 (All Data)

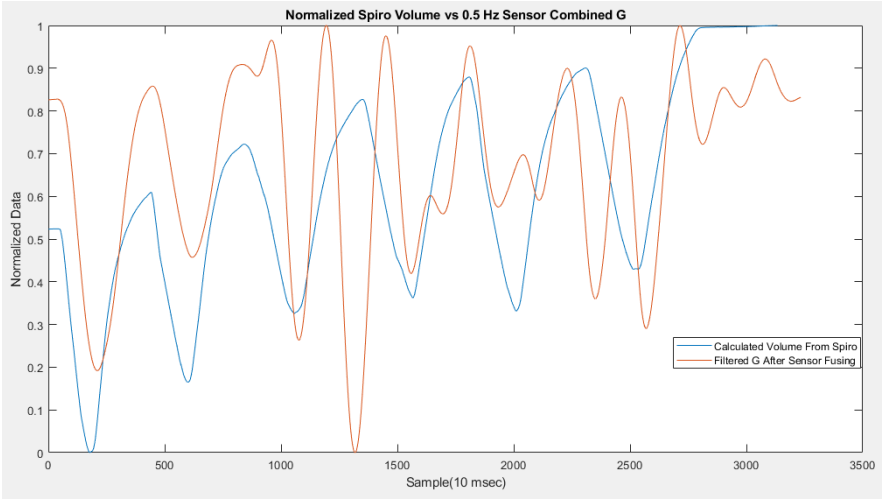

Figure 4.15. Comparison Between Sensor G Values And Fused G Values (Test 4).

Table 4.17. Scenario 2 Test 4 Peak and Valley Delays.

Cycles	**Peak to Peak Delay (ms)**	**Valley to Valley Delay (ms)**
Cycle 1	80 ms	320 ms
Cycle 2	70 ms	200 ms
Cycle 3	1170 ms	200 ms
Cycle 4	-1550 ms	Fake Valley
Cycle 5	Fake Peak	-80 ms
Cycle 6	40 ms	-780 ms
Cycle 7	-780 ms	Fake Valley
Cycle 8	Fake Peak	540 ms
Mean	615 ms	353 ms

Table 4.18. Scenario 2 Test 4 Respiration Rates and Correlation Coefficients.

Cycles	**$RR_{Accelerometer}$**	**$RR_{Spirometer}$**	**RR Error**	**Correlation Coef.**
Cycle 1-2	14.60 Cycle/min	14.56 Cycle/min	0.27 %	0.8029
Cycle 2-3	11.74 Cycle/min	14.96 Cycle/min	21.52 %	0.8504
Cycle 3-4	25.53 Cycle/min	11.83 Cycle/min	115.81 %	-0.0635
Cycle 4-5	23.35 Cycle/min	Fake Peak	*******	0.1646
Cycle 5-6	16.62 Cycle/min	13.07 Cycle/min	27.16 %	0.6298
Cycle 6-7	14.35 Cycle/min	12.00 Cycle/min	19.58 %	******
Cycle 7-8	25.71 Cycle/min	Fake Peak	*******	******
Mean	18.84 Cycle/min	13.28 Cycle/min	41.86 %	0.4460 (All Data)

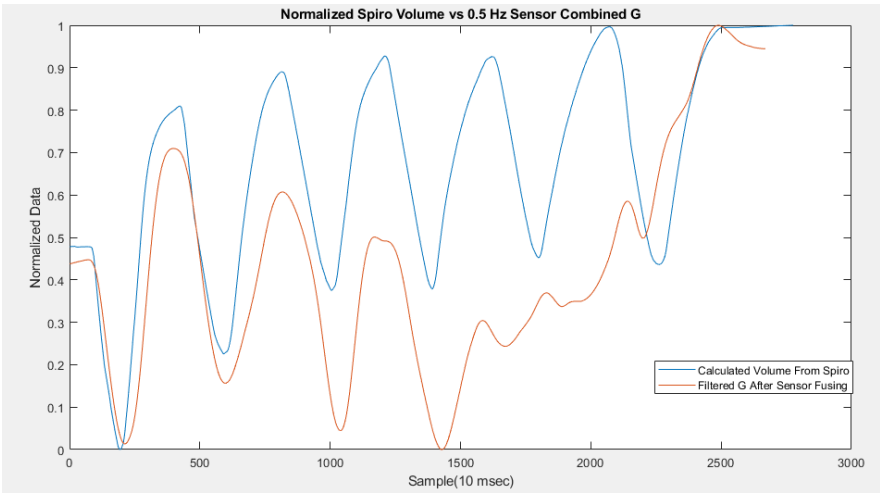

Figure 4.16. Comparison Between Sensor G Values And Fused G Values (Test 5).

Table 4.19. Scenario 2 Test 5 Peak and Valley Delays.

Cycles	**Peak to Peak Delay (ms)**	**Valley to Valley Delay (ms)**
Cycle 1	540 ms	180 ms
Cycle 2	-250 ms	60 ms
Cycle 3	10 ms	340 ms
Cycle 4	-400 ms	380 ms
Cycle 5	Not Detect	Not Detect
Cycle 6	700 ms	-600 ms
Mean	380 ms	312 ms

Table 4.20. Scenario 2 Test 5 Respiration Rates and Correlation Coefficients.

Cycles	$\mathbf{RR_{Accelerometer}}$	$\mathbf{RR_{Spirometer}}$	**RR Error**	**Correlation Coef.**
Cycle 1-2	18.40 Cycle/min	14.82 Cycle/min	24.16 %	0.9065
Cycle 2-3	14.35 Cycle/min	15.31 Cycle/min	6.27 %	0.8384
Cycle 3-4	16.95 Cycle/min	15.19 Cycle/min	11.59 %	0.7446
Cycle 4-5	Not Detect	14.53 Cycle/min	100.0 %	0.6928
Cycle 5-6	6.18 Cycle/min	13.93 Cycle/min	55.64 %	0.2194
Mean	13.97 Cycle/min	14.76 Cycle/min	5.35 %	0.6033 (All Data)

4 respiration cycles are missed in scenario 2 tests totally which means 86.20% success at finding peak points. 583 msec avarage delay is calculated for peak points. 27.36% respiration rate error is calculated when each cycle is considered one by one and 12.04% error is calculated when each test is considered as a whole window. Error is calculated as 100% in fake and not detecting peaks, therefore there is a big difference between two error percentages. 583 msec avarage peak to peak delay is calculated for scenario 2 tests. Correlation coefficient is calculated as 0.6845 when data is taken as peak to peak windows for all scenario 2 tests. 0.5861 is correlation coefficient when data is taken as whole window for each test.

There are 2 fake peaks and valleys in test 4. This means that periodic reciprocating motions affect system more than other moving types. It is clear that peak-valley differences are smaller than other tests in test 5 which means rotational movings absorbs changes in movement sensor originating from respiration.

SKLD values are calculated after all tests were completed. SKLD value is a good indicator to show similarity of two signals. Results which are closer to 0 means more similar signals. Table 4.21 shows SKLD values for scenario 1 and scenario 2 tests. Scenario 1 tests have smaller SKLD values than scenario 2 which means scenario 1 has more successful results than scenario 2.

Table 4.21. SKLD Values for Each Tests.

Test Name	**SKLD for Stable Body**	**SKLD for Moving Body**
Test 1	0.1613	0.3184
Test 2	0.1206	0.1602
Test 3	0.0824	0.2152
Test 4	0.0827	0.2375
Test 5	0.1402	0.2882
Mean	0.1174	0.2439

Table 4.22 shows peak delay percentages for each scenario. Delay percentages are calculated for each respiration cycle and they are averaged for each test. These values are calculated as

$$\text{DelayPercentage} = \frac{|Tps - Tpa|}{Tps - Tps'}. \tag{4.5}$$

T_{ps} means peak time for spirometer signal and T_{pa} means peak time for accelerometer signal. Peak time means starting point of new respiration cycle. According to results, 5.77 % average delay percentage for each respiration cycle in scenario 1 tests and 21.84% average delay percentage for each respiration cycle in scenario 2 tests are calculated.

Table 4.22. Peak to Peak Delay Difference Percentage for Each Test.

	Scenario 1	**Scenario 2**
Test 1	3.42 %	11.83 %
Test 2	6.78 %	17.76 %
Test 3	10.80 %	10.47 %
Test 4	3.48 %	39.97 %
Test 5	4.37 %	29.18 %
Average	5.77 %	21.84 %

5. CONCLUSION

In this thesis, an embedded system implementation for respiration pattern detection is proposed. Respiration rate which is an important vital sign for health condition of human body is calculated after finding respiration pattern. In chapter 2, several respiration rate detection methods are given. Two accelerometers are used to extract respiration pattern in this study. Using dual accelerometers is low a cost and easy to use system for respiration pattern detection and respiration rate calculation. This approach allows continuous monitoring of the respiratory system in terms of its respiration pattern.

In chapter 3, firstly, system architecture and used components are introduced. Data collected from 3-axis accelerometers is sent over bluetooth to MATLAB application using Atmega328 microcontroller. Secondly, algorithms developed and methodologies used are explained in this chapter. Test results and comparisons are introduced in Chapter 4. Tests are made in two scenearios and results are compared with ultrasonic based spirometer which is compatible with ATS/ERS standards. In the first scenario, test are performed with stable body. According to results, 260 msec mean delay 8.54% respiration rate error and 0.8280 correlation coefficient are calculated. Respiration rate error decreased to 2.99% when a given number of samples are averaged to calculate respiration rate. Additionally, all peak values corresponding to the starting point of inhalation are found in this scenario.

In the second scenario, test are performed with moving body. 583 msec delay, 27.36% respiration rate error and 0.6845 correlation coefficient are calculated. Respiration rate error decreased to 12.04% when a given number of samples are averaged to calculate respiration rate. The system has 86.20% success at finding peak points in scenario 2 tests. Higher error rates in moving body tests can be shown as a limitation of the implemented system.

In future works, different filtering techniques can be applied on the system to solve this limitation. Additionally, using different wireless communication technology like Wi-Fi gives a chance to build more complex or multi-patient systems. Accelerometer sensors can be incorporated into clothes as wearable instrumented smart clothes [23].

In conclusion, using movement sensors is one of the successful methodologies to extract respiration pattern. Two sensors is used in this system proved to operate more successfully than a single sensor. In real life applications, patients do not need to wear masks or belts while using movement sensors therefore this system can be used in sleep experiments and children.

REFERENCES

1. Preejith, S., A. Jeelani, P. Maniyar, J. Joseph and M. Sivaprakasam, "Accelerometer Based System for Continuous Respiratory Rate Monitoring", *2017 International Symposium on Medical Measurements and Applications*, pp. 171–176, 2017.

2. Ionescu, C. M., *The Human Respiratory System: An Analysis of the Interplay Between Anatomy, Structure, Breathing and Fractal Dynamics*, Springer Science & Business Media, 2013.

3. Ambekar, M. R. and S. Prabhu, "A Novel Algorithm to Obtain Respiratory Rate from the PPG Signal", *International Journal of Computer Applications*, Vol. 126, No. 15, 2015.

4. AL-Khalidi, F. Q., R. Saatchi, D. Burke, H. Elphick and S. Tan, "Respiration Rate Monitoring Methods: A Review", *Pediatric pulmonology*, Vol. 46, No. 6, pp. 523–529, 2011.

5. Aoki, H., Y. Takemura, K. Mimura and M. Nakajima, "Development of Non-Restrictive Sensing System for Sleeping Person Using Fiber Grating Vision Sensor", *Proceedings of 2001 International Symposium on Micromechatronics and Human Science*, pp. 155–160, 2001.

6. Greneker, E., "Radar sensing of heartbeat and respiration at a distance with applications of the technology", *Radar 97 (Conf. Publ. No. 449)*, pp. 150–154, 1997.

7. Hsu, C.-H. and J. C. Chow, "Design and Clinic Monitoring of a Newly Developed Non-Attached Infant Apnea Monitor", *Biomedical Engineering: Applications, Basis and Communications*, Vol. 17, No. 03, pp. 126–134, 2005.

8. Alkali, A. H., R. Saatchi, H. Elphick and D. Burke, "Facial Tracking in Thermal Images for Real-Time Noncontact Respiration Rate Monitoring", *2013 European*

Modelling Symposium, pp. 265–270, 2013.

9. Ciołek, M., M. Niedźwiecki, S. Sieklicki, J. Drozdowski and J. Siebert, "Automated Detection of Sleep Apnea and Hypopnea Events Based on Robust Airflow Envelope Tracking in the Presence of Breathing Artifacts", *Journal of biomedical and health informatics*, Vol. 19, No. 2, pp. 418–429, 2014.

10. Mazzanti, B., C. Lamberti and J. De Bie, "Validation of an ECG-Derived Respiration Monitoring Method", *Computers in Cardiology, 2003*, pp. 613–616, 2003.

11. Yıldırım, I., "Airflow Estimation from Respiratory Sounds", *Master's Thesis, Boğaziçi University*, 2013.

12. Ulukaya, S., G. Serbes, I. Sen and Y. P. Kahya, "A Lung Sound Classification System Based on the Rational Dilation Wavelet Transform", *2016 38th Annual International Conference of the Engineering in Medicine and Biology Society*, pp. 3745–3748, 2016.

13. Bates, A., M. J. Ling, J. Mann and D. K. Arvind, "Respiratory Rate and Flow Waveform Estimation from Tri-Axial Accelerometer Data", *2010 International Conference on Body Sensor Networks*, pp. 144–150, 2010.

14. Krehel, M., M. Schmid, R. M. Rossi, L. F. Boesel, G.-L. Bona and L. J. Scherer, "An Optical Fibre-Based Sensor for Respiratory Monitoring", *Sensors*, Vol. 14, No. 7, pp. 13088–13101, 2014.

15. Ertaş, G. and N. Gültekin, "Design of a Respiration Pattern Detecting Device based on Thoracic Motion Tracking with Complementary Filtering", *Süleyman Demirel Üniversitesi Fen Bilimleri Enstitüsü Dergisi*, Vol. 22, No. 1, pp. 32–37, 2018.

16. *MPU6050 Product Specification*, 2013, `https://invensense.tdk.com/products/motion-tracking/6-axis/`, accessed in June 2021.

17. Jiang, P. and R. Zhu, "Dual Tri-Axis Accelerometers for Monitoring Physiological Parameters of Human Body in Sleep", *2016 Sensors*, pp. 1–3, 2016.

18. Phan, D., "Estimating Confident Index of Respiratory Signal Using an Accelerometer", *2017 2nd International Conference on Signal and Image Processing*, pp. 413–417, 2017.

19. *HC-05 Bluetooth to Serial Port Module*, 2010, `https://components101.com/wireless/hc-05-bluetooth-module`, accessed in June 2021.

20. *Arduino Pro Mini Manual*, 2021, `https://docs.arduino.cc/`, accessed in June 2021.

21. Ciftci, K. and Y. P. Kahya, "Respiratory Airflow Estimation by Time Varying Autoregressive Modeling", *2008 30th Annual International Conference of the Engineering in Medicine and Biology Society*, pp. 347–350, 2008.

22. Yenen, S. D., F. Arikan and T. Gulyaeva, "Comparison of IRI-Plas STEC and IONOLAB-STEC Over a Midlatitude GPS Network", *2019 9th International Conference on Recent Advances in Space Technologies*, pp. 649–653, 2019.

23. Huang, C.-C., W.-Y. Lin and M.-Y. Lee, "Development and Verification of an Accelerometer-Based Respiratory Detection Algorithm with Wearable Instrumented Smart Clothes", *2017 International Conference on Systems, Man, and Cybernetics*, pp. 578–581, 2017.

APPENDIX A: HC-05 BLUETOOTH MODULE AT COMMANDS

Table A.1. AT Commands for HC-05.

Command	**Respond**	**Parameter**	**Description**
AT	OK	-	Test Command
AT+RESET	OK	-	Reset Command
AT+VERSION?	+VERSION:"P1" OK	P1: Firmware Version	Get Firmware Version
AT+ORGL?	OK	-	Set Default Parameters
AT+ADDR?	+ADDR:"P1" OK	P1: Address of Bluetooth Module	Get Module Address
AT+NAME ="P1"	OK	P1: Module Name	Set Module Name
AT+NAME?	+NAME:"P1" OK (FAIL)	P1: Bluetooth Module Name	Get Module Address (Default:HC-05)
AT+ROLE ="P1"	OK	P1: 0:Slave, 1:Master, 2:Slave-Loop	Set Module Mode
AT+ROLE?	+ROLE:"P1" OK	P1: 0:Slave, 1:Master, 2:Slave-Loop	Get Module Mode
AT+PSW ="P1"	OK	P1: Module PIN Code	Set Module PIN Code
AT+PSW?	+PSW:"P1" OK	P1: Bluetooth PIN Code	Get Module PIN Code (Default:1234)

Table A.1. AT Commands for HC-05. (cont.)

Command	**Respond**	**Parameter**	**Description**
AT+UART ="P1","P2","P3"	OK	P1: Baud P2: Stop Bit P3: Parity	Set Module Serial Parameters
AT+UART?	+UART ="P1","P2","P3"	P1: Baud P2: Stop Bit P3: Parity	Get Module Serial Parameters
AT+CMODE ="P1"	OK	P1:"0: Fixed Address" "1:Any Address" "2:Slave-loop"	Set Connect Mode
AT+CMODE?	+ CMODE:"P1" OK	P1:"0:Fixed Address" "1:Any Address" "2:Slave-loop"	Check Connect Mode
AT+STATE?	+STATE :"P1"	P1: "READY" "INITIALIZED" "PAIRABLE" "PAIRED" "INQUIRING" "CONNECTING" "CONNECTED" "DISCONNECTED" "NUKNOW"	Get Module Working State